PHYSICAL REVIEW E, VOLUME 64, 051806

Anisotropy effects of Hele-Shaw cells on viscous fingering instability in dilute polymer solutions

Masami Kawaguchi,* Yuhsuke Hibino, and Tadaya Kato
Department of Chemistry for Materials, Faculty of Engineering, Mie University, 1515 Kamihama, Tsu, Mie 514-8507, Japan

(Received 12 March 2001; published 23 October 2001)

We study the effect of anisotropy of the Hele-Shaw cell on the viscous fingering instability in dilute polymer solutions with shear thinning. In isotropic cells, the tip-splitting instability is observed at the same pressure gradient for a fixed polymer concentration, whereas in anisotropic cells the side oscillation instability occurs at higher pressure gradient than the tip-splitting instability. Narrowing of the finger width in the isotropic cell is well correlated with the tip-splitting instability, whereas the finger width in the anisotropic cell is almost independent of the sample. The modified Darcy's law, where the constant viscosity is replaced by the shear thinning viscosity, gives good agreement with the experiments, irrespective of the cell and the fluid.

DOI: 10.1103/PhysRevE.64.051806 PACS number(s): 61.41.+e

Viscous fingering instabilities in polymer solutions have attracted much attention in the past few decades [1,2]. Polymer solutions in a flow field can develop instability, which is attributable to their non-Newtonian behavior, viscoelasticity, shear thinning, shear thickening, yield stress, etc. Such rheological properties should strongly influence the formation of viscous fingering patterns in polymer solutions. Several shear thinning polymer solutions [3–11] and some viscoelastic ones [12–15] have been used for viscous fingering experiments and a variety of fingering patterns were observed. However, understanding the correlation between the rheological properties and the viscous fingering instability in polymer solutions is insufficient.

The effect of anisotropy of a Hele-Shaw cell on viscous fingering instabilities in polymer solutions is a challenging topic since only a few studies have been performed [10] and no qualitative understanding was obtained. For semidilute shear thinning polymer solutions in an anisotropic cell [10], the finger grew faster along a groove, the width of the finger was smaller, and a dendrite pattern was observed at higher velocities.

In this article, we describe viscous fingering experiments on dilute polymer solutions with weak shear thinning at 25 °C in isotropic and anisotropic linear Hele-Shaw cells to investigate the effect of anisotropy of the Hele-Shaw cell on the viscous fingering instability by taking into account the rheological properties of the polymer solutions. The cells are made of two float-glass plates separated by a thin rubber sheet spacer, fixing the gap $b = 0.05$ cm. The length L and the width W of the channel in the cell are fixed to be 20 and 3 cm, respectively. For the anisotropic cell the upper plate was a glass plate with a thin groove of triangular section of about 0.003 cm width and 0.001 cm depth from an inlet toward the unsealed edge. Air is injected at fixed pressures of 10, 15, 25, 45, and 90 cm H_2O, using the same pressure reservoir as described previously [5,8,10] to displace polymer solutions. The polymer solutions used are polystyrene (PS) with a molecular weight of 20×10^6 in dioctyl phthalate (DOP). The concentrations of PS in DOP solutions used are 0.0, 0.01, 0.1, 0.15, and 0.2 g/100 g, which are less than the overlap concentration of PS chains in DOP, 0.29 g/100 g and higher than those studied by Smith, Wu, Libchaber, Moses, and Witten [4]. The rheological data are measured using a Paar Physica MCR300 rheometer. When a stepwise and continuous increase in shear rate is applied to measure the steady state viscosity, the 0.01, 0.1, 0.15, and 0.2 g/100 g PS-DOP solutions show weak shear thinning and follow a nearly Newtonian flow as shown in Fig. 1. Except for the 0.01 g/100 g PS-DOP solution, the first normal stress differences N_1 due to the Wissenberg effect are observed above a shear rate of 40 s^{-1} for the 0.1 and 0.15 g/100 g and above a shear rate of 30 s^{-1} for the 0.2 g/100 g PS-DOP solutions leading to overshooting behavior. DOP shows Newtonian behavior as shown in Fig. 1. The surface tensions of the samples are obtained as 30.7, 29.1, 29.5, 29.5, and 29.0 mN/m in order of increasing PS concentration by the Wilhelmy plate method. The viscous fingering patterns are recorded with a charge-coupled device camera/recorder method.

The finger tip velocity V_t can be calculated from a plot of the distance L_f from the inlet to the tip of the grown finger against the necessary time. In the plot a straight portion is obtained for the distance $L_f = 5-6$ cm from the inlet and beyond that distance the plot data deviate positively from the initial straight line, irrespective of the injection pressure or the sample. The relative finger width λ defined by the ratio

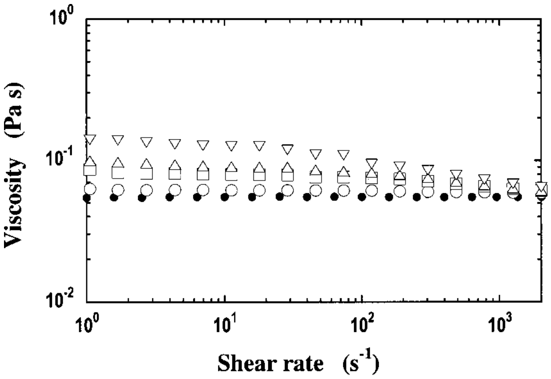

FIG. 1. Steady state viscosity data for DOP (●) and 0.01 (○), 0.1 (□), 0.15 (△), and 0.2 (▽) g/100 g DOP-PS solutions as a function of the shear rate.

---

*Author to whom correspondence should be addressed. FAX: 81-59-231-9471. Email address: kawaguti@chem.mie-u.ac.jp

1063-651X/2001/64(5)/051806(3)/$20.00

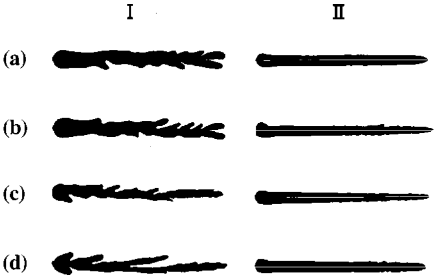

FIG. 2. Typical fingering patterns of 0.01 (a), 0.1 (b), 0.15 (c), and 0.2 (d) g/100 g DOP-PS solutions at the injection pressure of 45 cm H_2O in the isotropic (I) and anisotropic (II) Hele-Shaw cells. The finger length is 15 cm.

of the finger width and the cannel width W, is another important and characteristic quantity in understanding the finger pattern and the finger width can be calculated from the increase of the displaced area A by air in time t:$\lambda = (1/V_t)(dA/dt)/W$ [14]. Each plot of A against t has a straight portion for the distance L_f of 5–6 cm. Therefore, for the distance $L_f = 5-6$ cm the finger growth can be regarded as in steady state.

For DOP in the isotropic cell, the single finger is similar to a Saffman-Taylor finger, whereas in the anisotropic cell a narrower and more pointed finger is observed and its shape is similar to those for Newtonian fluids in a grooved linear Hele-Shaw cell [16]. Moreover, the DOP solvent shows no branched pattern for the injection pressure ranges studied here in either cell. In the isotropic cell each PS-DOP solution shows tip-splitting growth, irrespective of the injection pressure. Typical viscous fingering patterns of the 0.01, 0.1, 0.15, and 0.2 g/100 g PS-DOP solutions at the fixed injection pressure of 45 cm H_2O are displayed in Fig. 2. In the anisotropic cell the 0.01 g/100 g PS-DOP solution shows only a pointed finger pattern for the entire injection pressure range. The difference can be attributed to the fact that flow instability occurs at higher velocities since the fingers in the latter cell are more stable than those in the former cell. When the PS concentration is increased, tip splitting occurs at short distances from the inlet in the isotropic cell, whereas the finger in the anisotropic cell is a more pointed one with sides made less smooth by weak oscillations. Therefore, it seems that the tip-splitting and/or the side oscillation instabilities occur when the pressure gradient exceeds some value. The pressure gradient is defined by the ratio of the injection pressure and the distance $L - L_f$ between the finger tip and the outlet.

First, we estimate the pressure gradient at the onset of the tip splitting in the PS solutions. The onset pressure gradients for the 0.01, 0.1, 0.15, and 0.2 g/100 g PS-DOP solutions are obtained as 290, 126, 115, and 91 Pa/cm, respectively, irrespective of the injection pressure. This means that the tip-splitting instability appears when the value of V_t increases beyond a threshold tip velocity. From the value of V_t we can obtain the imposed shear rate of $2V_t/b$; the imposed shear rates at the threshold of the tip-splitting instability are obtained as 100, 45, 17, and 13 s^{-1} for the 0.01, 0.1, 0.15, and 0.2 g/100 g PS-DOP solutions, respectively. We note that these are close to the shear rates at the onset of shear thinning of the steady state viscosities for the corresponding PS-DOP solutions as shown in Fig. 1. The observed shear thinning behavior is due to the viscoelastic properties of the PS-DOP solution, leading to the tip-splitting instability. In other words, the PS chain used in the present study has a large size and it should yield viscoelastic normal forces even below the overlap concentration.

Furthermore, in a viscous fingering experiment, it is reasonable to consider that the fingering pattern should grow at the imposed shear rate. Thus, we tried to measure the values of N_1 for the PS-DOP solutions from a one-shot steady state viscosity measurement under nearly the same imposed shear rate as at the threshold of the tip-splitting instability, and values of N_1 less than 2–3 Pa were obtained. Thus we have shown experimentally that a viscoelastic normal force occurs at nearly the shear rate for the onset of the tip-splitting instability. In addition, the tip-splitting instability observed in the present study may be similar to that observed by Vlad and Maher [15], who investigated viscous fingering in Borger fluids, namely, constant viscosity elastic fluids.

On the other hand, in the anisotropic cell the finger instability corresponds to weak oscillation on the two sides of the finger as shown in Fig. 2. The shape can be classified as a dendrite pattern. However, the wavelength and amplitude of such side oscillations cannot be determined. Moreover, it is sometimes not easy to estimate the position where such a side oscillation instability first appears compared to the position where the tip-splitting instability occurs. The pressure gradients at the onset of the side oscillation instability range from 400 to 600 Pa/cm.

Next, we focus on the steady state finger tip velocity V_t defined by fitting an initial straight line to the plot of the distance L_f from the inlet to the tip of the grown finger as a function of time. In order to obtain the velocity V of the fluid far away from the finger, the V_t value can be modified by the finger width λ as follows: $V = V_t\lambda$. Such an average finger velocity V can be related to Darcy's law $V = (b^2/12\eta)\nabla p$, where η is the viscosity and ∇p is the pressure gradient. Moreover, in order to test Darcy's law for non-Newtonian fluids, we should replace the constant viscosity η by an effective viscosity η_{eff} at the imposed shear rate defined by $2V_t/b$ [11,17,18]. Thus, the modified Darcy's law can be defined as $V = (b^2/12\eta_{\mathrm{eff}})\nabla p$ and the η_{eff} value can be obtained from interpolation of a plot of the steady state viscosity against the shear rate as shown in Fig. 1. In Fig. 3 the values of V for steady state finger growth are plotted against the value of $(\nabla p/\eta_{\mathrm{eff}})$ and the dashed straight line drawn in the figure corresponds to the value of $(b^2/12)$, where the pressure gradient is calculated by putting $L_f = 5$ cm. The fit of the resulting data to the modified Darcy's law is good, irrespective of the cell and the fluid.

The relative finger width λ is well known to be related to the dimensionless parameter $1/B = 12(\eta_{\mathrm{eff}}, V_t/\gamma)(W/b)^2$ [19,20], where γ is the surface tension of the displaced, more viscous fluid. The values of λ in steady state of finger growth are plotted against $1/B$ in Fig. 4. The λ values in the isotropic cell are larger than those in the anisotropic cell and they tend to approach a plateau value of ca. 0.35 at higher velocities, although they are somewhat scattered. Moreover, the λ pla-

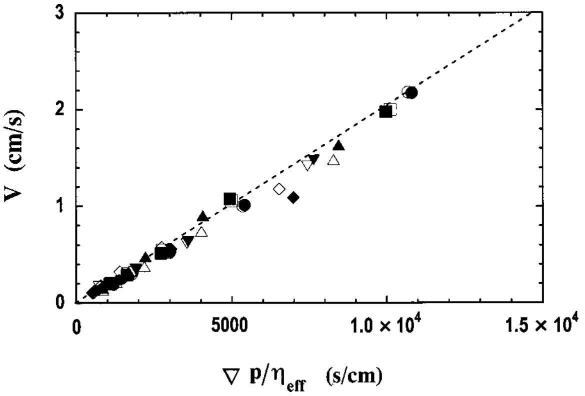

FIG. 3. Plots of V for DOP (circles), 0.01 (squares), 0.1 (up triangles), 0.15 (down triangles), and 0.2 (diamonds) g/100 g DOP-PS solutions as a function of $\nabla p/\eta_{\mathrm{eff}}$ in the isotropic (open symbols) and anisotropic (filled symbols) Hele-Shaw cells. The dashed straight line has a slope of $(b^2/12)$.

teau value for the PS-DOP solutions is clearly smaller than the λ value of 0.5 for the solvent DOP. This can be well correlated with the finger pattern morphology, namely, all PS-DOP solutions show a tip-splitting pattern. Moreover, the viscous finger narrowing for a shear thinning polymer solution qualitatively agrees with the theoretical prediction of Poire and Ben Amar [21].

In the anisotropic cell, on the other hand, the λ values can be almost fitted with a smooth curve, irrespective of the sample, and it approaches a plateau value of ca. 0.25. The smaller plateau value of λ may be mainly attributed to the fact that the effects of anisotropy of the Hele-Shaw cell suppress the tip-splitting instability due to the faster finger growth along the groove.

In conclusion, we have demonstrated viscous fingering instability of dilute polymer solutions with weak shear thinning in isotropic and anisotropic linear Hele-Shaw cells. Tip-splitting and side oscillation instabilities are observed in isotropic and anisotropic cells, respectively. The former instability occurs at the same pressure gradient for fixed polymer concentration and it can be related to the onset of shear thinning due to viscoelastic normal forces. The average finger velocity data are in good agreement with a modified Darcy's law, irrespective of the cell. Narrowing of the finger in the isotropic cell is induced by the tip-splitting instability, whereas the finger width in the anisotropic cell is independent of the sample.

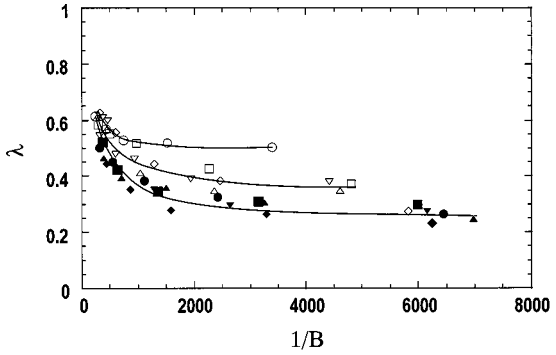

FIG. 4. Plots of λ for DOP and for 0.01, 0.1, 0.15, and 0.2 g/100 g DOP-PS solutions as a function of $1/B$ in the isotropic and anisotropic Hele-Shaw cells. Symbols in the figure are the same as in Fig. 3. The solid lines are guides for the eye.

This work was partially supported by Grant-in-Aid for Scientific Research on Priority Area (A) ''Dynamic Control of Strongly Correlated Soft Materials'' (No. 413/13031045) from the Ministry of Education, Science, Sports, Culture and Technology.

[1] K. V. McCloud and J. V. Maher, Phys. Rep. **260**, 139 (1995).
[2] P. Meakin, *Fractals, Scaling and Growth Far from Equilibrium* (Cambridge University Press, Cambridge, 1998), p. 388.
[3] G. Daccord, J. Nittmann, and H. E. Stanley, in *On Growth and Form*, edited by H. E. Stanley and N. Ostrowsky (Martinus Nijhoff, Dordrecht, 1986), p. 203.
[4] D. E. Smith, X. Z. Wu, A. Libchaber, E. Moses, and T. Witten, Phys. Rev. A **45**, R2165 (1992).
[5] K. Makino, M. Kawaguchi, K. Aoyama, and T. Kato, Phys. Fluids **7**, 455 (1995).
[6] D. Bonn, H. Kellay, M. Ben Amar, and J. Meunier, Phys. Rev. Lett. **75**, 2132 (1995).
[7] T. Yamamoto, H. Kamikawa, and K. Nakamura, Nippon Reoroji Gakkaishi **24**, 105 (1996).
[8] M. Kawaguchi, K. Makino, and T. Kato, Physica D **105**, 121 (1997); **107**, 325 (1997).
[9] D. Bonn and J. Meunier, Phys. Rev. Lett. **79**, 2662 (1997).
[10] M. Kawaguchi, A. Shibata, K. Shimomoto, and T. Kato, Phys. Rev. E **58**, 785 (1998); M. Kawaguchi, K. Shimomoto, A. Shibata, and T. Kato, Chaos **9**, 323 (1999).
[11] A. Lindner, D. Bonn, and J. Meunier, Phys. Fluids **12**, 256 (2000).
[12] H. Zhao and J. V. Maher, Phys. Rev. A **45**, R8328 (1992); Phys. Rev. E **47**, 4278 (1993).
[13] J. Ignes-Mullol, H. Zhao, and J. V. Maher, Phys. Rev. E **51**, 1338 (1995).
[14] D. H. Vlad, J. Inges-Mullol, and J. V. Maher, Phys. Rev. E **60**, 4423 (1999).
[15] D. H. Vlad and J. V. Maher, Phys. Rev. E **61**, 5439 (2000).
[16] M. Rabaud, Y. Couder, and N. Gerard, Phys. Rev. A **37**, 935 (1988).
[17] L. Kondic, P. Palffy-Muhoray, and M. J. Shelley, Phys. Rev. E **54**, R4536 (1996).
[18] M. Kawaguchi, Macromol. Symp. **160**, 85 (2000).
[19] D. Bensimon, L. P. Kadanoff, S. Liang, B. I. Shariman, and C. Tang, Rev. Mod. Phys. **58**, 977 (1986).
[20] P. Tabeling, G. Zocchi, and A. Libchaber, J. Fluid Mech. **177**, 67 (1987).
[21] E. C. Poire and M. Ben Amar, Phys. Rev. Lett. **81**, 2048 (1998).